Vol. **110** (2006) *ACTA PHYSICA POLONICA A* No. 3

Proceedings of the XXXV International School of Semiconducting Compounds, Jaszowiec 2006

Quantized Absorption Strength of Multi-Exciton Quantum Dots

K. Wójcik, A. Grodecka and A. Wójs

Institute of Physics, Wrocław University of Technology
Wybrzeże Wyspiańskiego 27, 50-370 Wrocław, Poland

Energy and absorption/recombination spectra of up to two electron–hole pairs confined in a spherical quantum dot are studied numerically as a function of dot radius (i.e., confinement volume). The transition between fermionic and bosonic behavior of the confined excitons is identified in coincidence with enhancement of low-energy absorption strength.

PACS numbers: 73.22.–f, 78.67.Hc, 71.35.–y

1. Introduction

Being bound states of two fermions, the excitons (X = e + h) can in some situations behave like bosons [1, 2]. A spectacular example is their Bose-Einstein condensation [3, 4], recently demonstrated [5] in a two-dimensional coupled quantum well. However, when excitons are confined in small quantum dots [6], spatial quantization of their e and h constituents exceeds excitonic binding. In consequence, the multi-exciton ground states in such systems are determined by Pauli exclusion principle applied to the individual fermionic constituents [7]. This can be expressed in terms of effective Pauli blocking for the excitons themselves, observed experimentally in photoluminescence studies showing population of consecutive excitonic shells as a function of increasing excitation power [8]. E.g., the lowest (s-) shell of a spherical dot can only hold two excitons (including spin), the next (p-) shell can hold six excitons, etc. In contrast, the allowed population of the exciton ground state without confinement is macroscopic (proportional to the real-space volume). Motivated by recent modulation reflectivity experiments [9], in this paper we study transition between those two extremes, i.e., collapse of the exciton Pauli blocking effect as a function of the dot size. In particular we seek a signature of this collapse in enhancement of the ground-state oscillator strength (i.e., low-energy absorption).

2. Model

We use a very simple model for a quantum dot with a variable volume (or area): an ideal spherical surface of radius R. While we concentrate on a

general effect, this model might be adequate to two-component semiconductor nanocrystals (with material with a narrower band gap deposited in a form of a thin layer around a spherical nanocrystal of a material with a larger band gap). The dot radius R is to be compared with a characteristic dimension of an exciton, i.e., effective Bohr radius $a_{\mathrm{B}} = \epsilon\hbar^2/\mu e^2$. Here, $\mu = (m_{\mathrm{e}}^{-1} + m_{\mathrm{h}}^{-1})^{-1} = m_{\mathrm{e}}/(1 + r^{-1})$ is the exciton reduced mass for a given mass ratio $r = m_{\mathrm{h}}/m_{\mathrm{e}}$. This leads to a dimensionless dot size, $s = R/a_{\mathrm{B}}$. The characteristic quantization energies $\varepsilon_l = \hbar^2 l(l+1)/2m_\alpha R^2$ (α = e or h) must be compared to the effective excitonic Rydberg, $Ry = e^2/2\epsilon a_{\mathrm{B}}$, yielding, e.g. $\varepsilon_1^{(\mathrm{e})}/Ry = 2s^{-2}/(1 + r^{-1})$.

The one- and two-exciton spectra are obtained from exact diagonalization of e + h or 2e + 2h Coulomb Hamiltonians in the configuration–interaction (CI) basis. The single-particle states are standard spherical harmonics $Y_l^m(\theta, \phi)$, labeled by angular momentum quantum numbers l and m, allowing for analytical expression of the two-body matrix elements. The X and 2X eigenstates are labeled by total angular momentum L, related to the wave vector $k = L/R$. In such numerical calculation the major source of error is the restriction of single-particle basis to a number of lowest shells ($l \leq l_{\max}$), accurate only for sufficiently small s.

3. Results and discussion

3.1. One exciton

We begin with one exciton. The energy spectra for $r = 1$ and different values of s are shown in Fig. 1. For $s = \frac{1}{4}$ the low-energy spectrum can be predicted from addition of e and h angular momenta, assuming both particles in their low-energy shells (although due to the $r = 1$ symmetry, degeneracy of the e $\leftrightarrow$ h symmetric states is removed by interaction at arbitrarily small s). This is the small dot regime. For $s = 5$ (vanishing confinement regime) the lowest-energy band is a well-developed exciton dispersion. The intermediate frames show the transition.

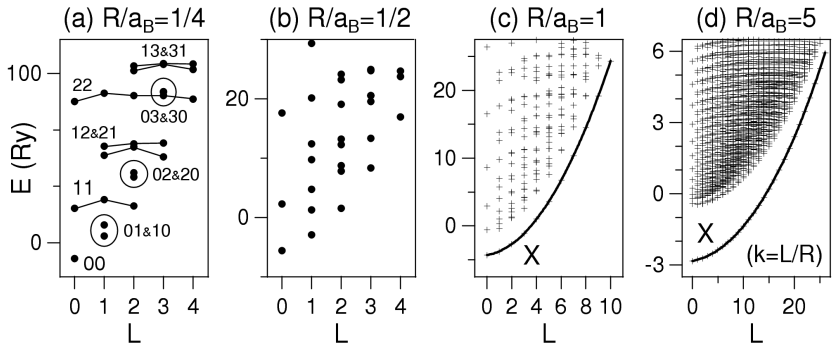

Fig. 1. Energy spectra of one e–h pair in spherical quantum dots of different radii R, calculated for the mass ratio $m_{\mathrm{h}}/m_{\mathrm{e}} = 1$ and including single-particle angular momentum shells with $l \leq 15$. Ry is Rydberg; a_{B} is Bohr radius. In (a) the lowest eigenstates are connected into bands labeled by e and h angular momenta ($l_{\mathrm{e}} l_{\mathrm{h}}$).

In Fig. 2 we show similar spectra for $r = 5$. Broken e $\leftrightarrow$ h symmetry rearranges the energy spectrum of a small dot, but the familiar excitonic dispersion of Fig. 1a is restored when the confinement is removed.

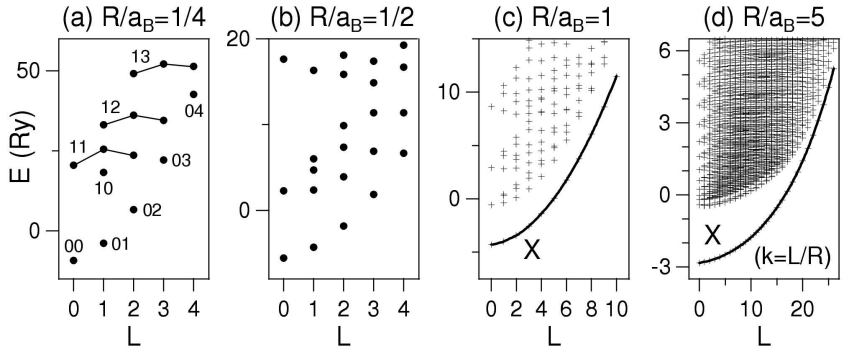

Fig. 2. The same as Fig. 1, but for the mass ratio $m_{\rm h}/m_{\rm e} = 5$.

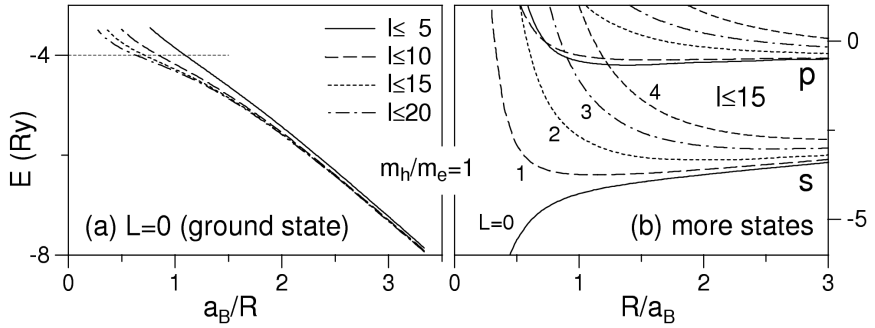

Fig. 3. (a) Ground state energy E of an e–h pair as a function of inverse dot radius R^{-1}, calculated for $m_{\rm h} = m_{\rm e}$ and for different numbers of included angular momentum shells. (b) Size dependence of different energy levels obtained for $l \leq 15$.

The continuous size-dependence of the energy levels is shown in Fig. 3. For $s^{-1} \to 0$ the ground state energy must converge to $-4Ry$ of a free 2D exciton. Figure 3a gives an idea about the number of shells that must be included in a CI calculation at a given s. Clearly, while the overall structure of the spectra in Figs. 1d and 2d appear correct, their absolute energy positions are very inaccurate. Figure 3b shows the development of excitonic s and p states when confinement weakens (within each band, different L's refer to the center-of-mass motion).

The excitonic oscillator strengths ω are shown in Fig. 4. Only the $L = 0$ states are optically active. In small dots, the distribution of ω among different $L = 0$ states (i.e., among the shells) is determined by overlaps of the relevant single-particle e and h orbitals. When confinement weakens, the excitonic correlation

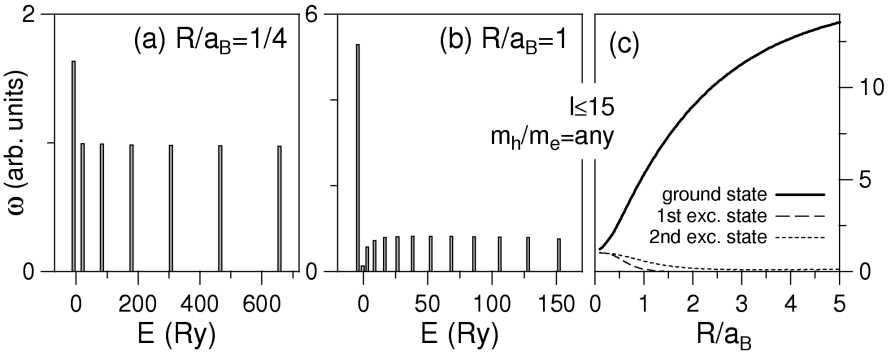

Fig. 4. (a,b) Absorption spectra (oscillator strength ω vs. energy E) of one e–h pair in spherical dots of different radii R. (c) Dependence of oscillator strengths for the three lowest optically active ($L = 0$) states on dot radius R.

emerges in the $L = 0$ ground state, to which also most of the oscillator strength is continuously transferred from the higher states. This also leads to the strong enhancement of the ground state.

3.2. Two excitons

The 2e + 2h energy spectra for different dot sizes s are shown in Fig. 5 ($r = 1$, symmetric case) and Fig. 6 ($r = 5$, more realistic case). As for a single exciton, only in small dots the spectra are very sensitive to the mass ratio r (and they can be understood by addition of angular momenta of four constituent fermions). However, in contrast to a single-exciton, recombination in a coupled two-exciton system can now occur also from $L \neq 0$ states. The oscillator strengths ω are indicated in Figs. 5 and 6 by diameters of circles drawn around each energy level.

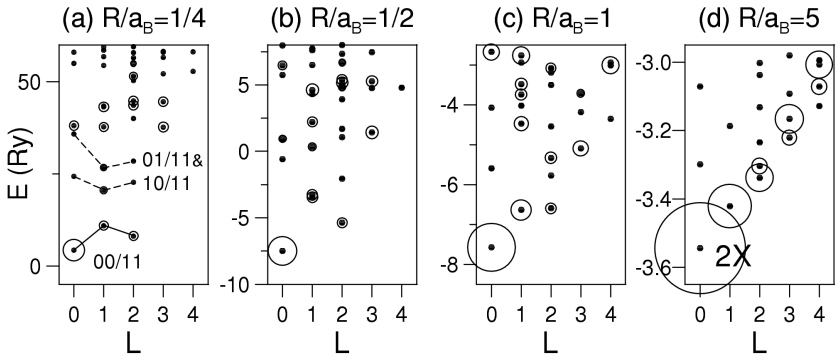

Fig. 5. Energy spectra of two e–h pairs in spherical quantum dots of different radii R, calculated for $m_{\rm h} = m_{\rm e}$ and including angular momentum shells with $l \leq 6$. Oscillator strength ω of each state is proportional to circle diameter. In (a), lowest eigenstates are labeled by e and h angular momenta $(l_{\rm e}l_{\rm h}/l'_{\rm e}l'_{\rm h})$.

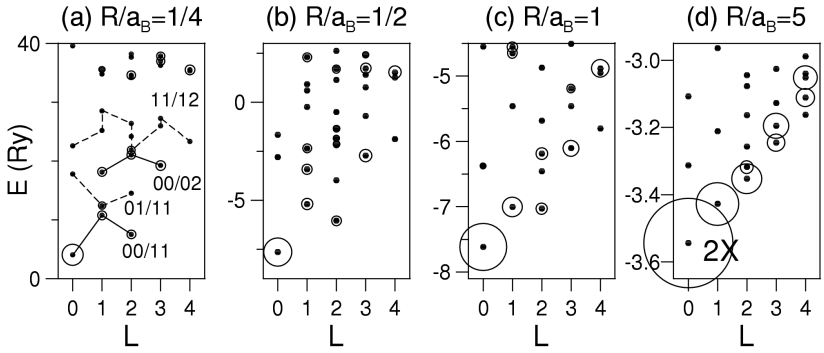

Fig. 6. The same as Fig. 5, but for the mass ratio $m_{\rm h}/m_{\rm e} = 5$.

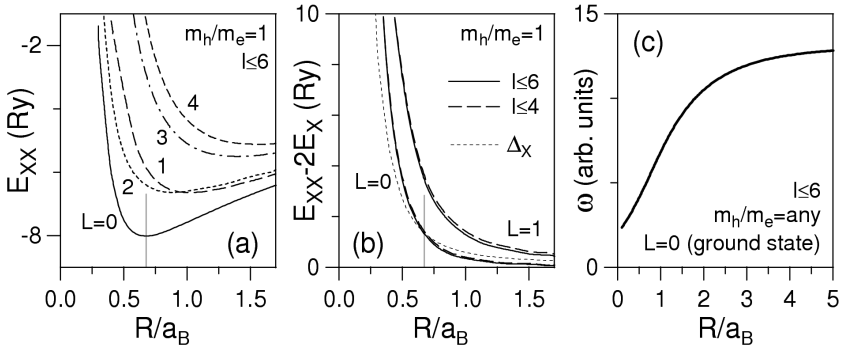

Fig. 7. (a) Lowest energy levels E at different angular momenta L of two e–h pairs as a function of dot radius R, calculated for $m_{\rm h} = m_{\rm e}$ and $l \leq 6$. (b) Two-pair energies E measured from two one-pair ground state energies $E_{\rm X}$ for $l \leq 4$ and $l \leq 6$. (c) Size dependence of oscillator strength ω of the two-pair ground state.

The continuous size-dependences extracted from those spectra is presented in Fig. 7. Frame (a) shows the size-evolution of the lowest energy levels at a few different angular momenta. Competition of kinetic energy and e–h attraction leads to a minimum in ground state energy $E_{\rm XX}$ at $s \approx 0.65$. Frame (b) shows $\delta_{\rm XX} = E_{\rm XX} - 2E_{\rm X}$ to compare one- and two-exciton ground states. This quantity is also compared with the excitation gap of a single exciton, $\Delta_{\rm X} = E^*_{\rm X} - E_{\rm X}$ (here, $E^*_{\rm X}$ is the energy of the exciton's first excited state). Coincidentally, the value of $s \approx 0.65$ determines the dot size beyond which $\delta_{\rm XX} < \Delta_{\rm X}$, i.e., $E_{\rm XX} < E_{\rm X} + E^*_{\rm X}$. This marks onset of effective attraction between excitons filling two lowest single--exciton states. Alternatively, this can be interpreted as crossover into the regime in which excitons no longer obey the effective Pauli exclusion principle and begin to populate single-exciton states like (weakly interacting) bosons. Frame (c) shows an increase of the ground-state oscillator strength ω with disappearing confinement, similar to the excitonic dependence in Fig. 4c.

4. Conclusion

In a very simple model, we studied numerically the transition of one- and two-exciton energy and recombination spectra as a function of confinement volume (or area). The crossover is identified from the small-dot regime (with the excitons filling single-exciton states in accordance with effective Pauli exclusion principle inherited from constituent fermions) to the unconfined regime (with many excitons at falling into the same energy state).

Acknowledgment

The authors gratefully acknowledge discussions with J. Misiewicz and G. Sęk. Work supported by grant No. 2P03B08525 of the Ministry of Science and Higher Education (Poland).

References

[1] S. Okumura, T. Ogawa, *Phys. Rev. B* **65**, 035105 (2002).

[2] M. Combescot, O. Betbeder-Matibet, *Europhys. Lett.* **59**, 579 (2002).

[3] L.V. Keldysh, A.N. Kozlov, *Zh. Eksp. Teor. Fiz.* **54**, 978 (1968) [*Sov. Phys. JETP* **27**, 521 (1968)].

[4] E. Hanamura, H. Haug, *Phys. Rep.* **33**, 209 (1977).

[5] L.V. Butov, A.C. Gossard, D.S. Chemla, *Nature* **418**, 751 (2002).

[6] L. Jacak, P. Hawrylak, A. Wójs, *Quantum Dots*, Springer, Berlin 1998.

[7] A. Wójs, P. Hawrylak, *Solid State Commun.* **100**, 487 (1996).

[8] S. Raymond, S. Fafard, P. Poole, A. Wójs, P. Hawrylak, S. Charbonneau, D. Leonard, R. Leon, P.M. Petroff, J.L. Merz, *Phys. Rev. B* **54**, 11548 (1996).

[9] P. Podemski, G. Sek, R. Kudrawiec, A. Wójs, J. Misiewicz, B. Alloing, L.H. Li, A. Fiore, A. Somers, J.P. Reithmaier, A. Forchel, to be published.